

REPORT DOCUMENTATION PAGE			Form Approved OMB No. 0704-0188	
<small>Public reporting burden for this collection of information is estimated to average 1 hour per response, including the time for reviewing instructions, searching existing data sources, gathering and maintaining the data needed, and completing and reviewing the collection of information. Send comments regarding this burden estimate or any other aspect of this collection of information, including suggestions for reducing this burden, to Washington Headquarters Services, Directorate for Information Operations and Reports, 1215 Jefferson Davis Highway, Suite 1204, Arlington, VA 22202-4302, and to the Office of Management and Budget, Paperwork Reduction Project (0704-0188), Washington, DC 20503.</small>				
1. AGENCY USE ONLY (Leave blank)		2. REPORT DATE 23 May 1998	3. REPORT TYPE AND DATES COVERED Technical	
4. TITLE AND SUBTITLE Nanocrystalline Aluminum Nitride and Aluminum/Gallium Nitride Nanocomposites via Transamination of $[M(NMe_2)_3]_2$, $M = Al, Al/Ga (1/1)$			5. FUNDING NUMBERS N00014-95-1-0194 R&T Project 3135008---16 Dr. Harold E. Guard	
6. AUTHOR(S) J. F. Janik, R. L. Wells, J. L. Coffey, J. V. St. John, W. T. Pennington, and G. L. Schimek				
7. PERFORMING ORGANIZATION NAME(S) AND ADDRESS(ES) Department of Chemistry Duke University Durham, NC 27708-0346			8. PERFORMING ORGANIZATION REPORT NUMBER Technical Report No. DU/DC/TR-75	
9. SPONSORING / MONITORING AGENCY NAME(S) AND ADDRESS(ES) Office of Naval Research 300 North Quincy Street Arlington, VA 22217-5000			10. SPONSORING / MONITORING AGENCY REPORT NUMBER	
11. SUPPLEMENTARY NOTES Accepted for publication in the <i>Chemistry of Materials</i>			<div style="font-size: 2em; transform: rotate(-10deg); position: relative; top: -50px; left: 50px;">19980601 059</div>	
12a. DISTRIBUTION / AVAILABILITY STATEMENT Approved for Public Release Distribution Unlimited			12b. DISTRIBUTION CODE	
13. ABSTRACT (Maximum 200 words) Reactions of $[Al(NMe_2)_3]_2$ with NH_3 , mimicking the case of the related Ga-derivative, provided an Al-amide-imide precursor that was pyrolyzed to pure nanocrystalline AlN. Based on that chemistry, a mixed Al/Ga precursor system was designed to lead to the bimetallic nitride composites. A prototype study included equilibration in hexane or toluene of the dimers $[M(NMe_2)_3]_2$, $M = Al, Ga$, which resulted in the formation of homoleptic four-membered ring compound $(Me_2N)_2Al(\mu-NMe_2)_2Ga(NMe_2)_2$. Crystalline $[M(NMe_2)_3]_2$, $M = Al/Ga (1/1)$, obtained from this equilibration was structurally characterized. Transamination/deamination reactions carried out with liquid NH_3 in the pre-equilibrated bimetallic system $[Al(NMe_2)_3]_2/[Ga(NMe_2)_3]_2$, $Al/Ga = 1/1$, resulted in the mixed M-amide-imide precursors that were converted at 700 to 1100 °C to aluminum/gallium nitride nanocomposite materials. The nature of these bulk nanocomposites has been elucidated by XRD, TEM/EDS, IR, and PL techniques.				
14. SUBJECT TERMS Al-amide-imide, transamination/deamination, mixed metal-amide-imide aluminum/gallium nitride, nanocomposite			15. NUMBER OF PAGES 32	
			16. PRICE CODE	
17. SECURITY CLASSIFICATION OF REPORT Unclassified	18. SECURITY CLASSIFICATION OF THIS PAGE Unclassified	19. SECURITY CLASSIFICATION OF ABSTRACT Unclassified	20. LIMITATION OF ABSTRACT Unlimited	

OFFICE OF NAVAL RESEARCH

Grant N00014-95-1-0194
R&T Project 3135008---16

Dr. Harold E. Guard

Technical Report No. DU/DC/TR-75

**Nanocrystalline Aluminum Nitride and Aluminum/Gallium Nitride
Nanocomposites via Transamination of $[M(NMe_2)_3]_2$, $M = Al, Al/Ga$ (1/1)**

Jerzy F. Janik and Richard L. Wells
Department of Chemistry, Paul M. Gross Chemical Laboratory, Duke University
Durham, NC 27708-0346

Jeffery L. Coffey and John V. St. John
Department of Chemistry, Texas Christian University, Ft. Worth, TX 76129

William T. Pennington and George L. Schimek
Department of Chemistry, Clemson University, Clemson, South Carolina 29634

Accepted for Publication in *Chemistry of Materials*

Duke University
Department of Chemistry,
P. M. Gross Chemical Laboratory
Box 90346
Durham, NC 27708-0346

23 May 1998

Reproduction in whole or in part is permitted for any purpose of the United States Government.

This document has been approved for public release and sale; its distribution is unlimited.

DTIC QUALITY INSPECTED 3

**Nanocrystalline Aluminum Nitride and Aluminum/Gallium Nitride
Nanocomposites via Transamination of $[M(NMe_2)_3]_2$, $M = Al, Al/Ga$ (1/1)**

Jerzy F. Janik[†] and Richard L. Wells*

Department of Chemistry, Paul M. Gross Chemical Laboratory, Duke University
Durham, NC 27708-0346

Jeffery L. Coffey and John V. St. John

Department of Chemistry, Texas Christian University, Ft. Worth, TX 76129

William T. Pennington and George L. Schimek

Department of Chemistry, Clemson University, Clemson, South Carolina 29634

Abstract. Reactions of $[Al(NMe_2)_3]_2$ with NH_3 , mimicking the case of the related Ga-derivative, provided an Al-amide-imide precursor that was pyrolyzed to pure nanocrystalline AlN. Based on that chemistry, a mixed Al/Ga precursor system was designed to lead to the bimetallic nitride composites. A prototype study included equilibration in hexane or toluene of the dimers $[M(NMe_2)_3]_2$, $M = Al, Ga$, which resulted in the formation of homoleptic four-membered ring compound $(Me_2N)_2Al(\mu-NMe_2)_2Ga(NMe_2)_2$. Crystalline $[M(NMe_2)_3]_2$, $M = Al/Ga$ (1/1), obtained from this equilibration was structurally characterized. Transamination/deamination reactions carried out with liquid NH_3 in the pre-equilibrated bimetallic system $[Al(NMe_2)_3]_2/[Ga(NMe_2)_3]_2$, Al/Ga = 1/1, resulted in the mixed M-amide-imide precursors that were converted at 700 to 1100 °C to aluminum/gallium nitride nanocomposite materials. The nature of these bulk nanocomposites has been elucidated by XRD, TEM/EDS, IR, and PL techniques.

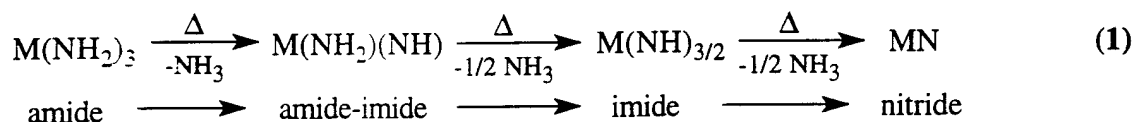
* Correspondence to: R. L. Wells

[†] On leave from the University of Mining and Metallurgy, Krakow, Poland

Introduction

Some group 13 nitrides such as BN and AlN are promising ceramic materials¹ and others are advantageous semiconductors² with a direct bandgap from 1.4 eV (InN) to 3.4 eV (GaN), and to 6.2 eV (AlN). However, new technological applications require materials with tunable electronic/crystalline properties and improved ceramic features. For example, the first demand is encountered in advanced blue LEDs and blue laser designs which employ nitride's solid solution films with appropriate crystalline properties.² On the ceramic application side, nitride solid solutions and composite materials are expected to possess unique and often improved properties over pure components.^{1b, 3} In this regard, it is generally recognized that classical bulk syntheses of these materials have intrinsic limitations to achieve many of the challenging goals and the problems' solutions are sought in precursor design and thermoprocessing.

We recently demonstrated that transamination/deamination reactions at ambient conditions between $[\text{Ga}(\text{NMe}_2)_3]_2$ and NH_3 afforded the gallium imide, $[\text{Ga}(\text{NH})_{3/2}]_n$, that was pyrolyzed to high purity nanocrystalline GaN.⁴ Related chemistry has also been reported for making thin films of such main-group nitrides as GaN^{5a} , AlN^{5b} , $\text{Si}_3\text{N}_4^{5c}$, and $\text{Sn}_3\text{N}_4^{5d}$. In all of these systems, it is convenient to think that the primary transamination product, the transient and unstable metal (M) amide, $\text{M}(\text{NH}_2)_x$, undergoes a stepwise elimination-condensation process, deamination, as illustrated for group 13 in equation 1:



Whereas at ambient conditions for $\text{M} = \text{Ga}$ the elimination approaches the polymeric imide stage, there is evidence that for $\text{M} = \text{Al}$,^{6a, b} Sn^{6c} a room temperature stable form could be close to the polymeric amide-imide, $[\text{M}(\text{NH}_2)(\text{NH})]_n$. In practice, as the crosslinking of

the M–N network progresses into the condensed solid phase, the deamination may encounter severe kinetic barriers to reach any of the distinct stages. This may result in precursors with entrapped residual NR_2 groups. Appropriate pyrolysis conditions, such as a NH_3 atmosphere, could then be used to minimize residual carbon in the nitride material.

The chemistry outlined above provokes an interesting idea of a bimetallic (or higher) group 13-amide-imide precursor from a solution-mixed molecular system $[\text{M}(\text{NR}_2)_3]_2/[\text{M}'(\text{NR}_2)_3]_2$. In a favorable case of efficiently coupled $\text{M}-\text{N}(\text{R}_2)-\text{M}'$ linkages, transamination with NH_3 , and the resultant transient NH_2 functionalities, could lead *via* deamination to homogeneously dispersed and crosslinked $\text{M}-\text{N}(\text{H})-\text{M}'$ bonds. The molecular level of homogeneity of such a mixed precursor coupled with abundant NH_2/NH M-bonded groups would present an outstanding opportunity for conversion to molecularly mixed nitrides. In this regard, hexagonal forms of AlN and GaN are known to form solid solutions for a full range of compositions, at least in AlGaN thin films from vapor deposition and molecular beam epitaxy techniques.^{2, 7} On the other hand, GaN and InN appear to form a more complex binary system with a miscibility gap.⁸

Herein, we first describe a successful preparation at ambient conditions of the solid Al-amide-imide from the transamination/deamination in the $[\text{Al}(\text{NMe}_2)_3]_2/\text{NH}_3$ system. This advantageous precursor was converted to high purity, bulk nanocrystalline AlN . Further, we discuss equilibration in hydrocarbon and aromatic solvents of the bimetallic system, $[\text{Al}(\text{NMe}_2)_3]_2/[\text{Ga}(\text{NMe}_2)_3]_2$, that results in the formation of the novel equilibrated four-membered ring compound $(\text{Me}_2\text{N})_2\text{Al}(\mu\text{-NMe}_2)_2\text{Ga}(\text{NMe}_2)_2$ which has been characterized by NMR spectroscopy. Transamination/deamination reactions with NH_3 were performed in the mixed system $[\text{Al}(\text{NMe}_2)_3]_2/[\text{Ga}(\text{NMe}_2)_3]_2$ to yield homogeneous Al/Ga-amide-imide precursors that were pyrolyzed to bulk aluminum/gallium nitride nanocomposites.

Experimental Section

General Techniques. All experiments were performed using standard vacuum/Schlenk techniques. Solvents were distilled from Na benzophenone ketyl or Na/K alloy prior to use. $[\text{Ga}(\text{NMe}_2)_3]_2$ ^{9a} and $[\text{Al}(\text{NMe}_2)_3]_2$ ^{9b} were prepared by literature methods. Anhydrous NH_3 over Na was transferred to a reaction vessel at -196 or -78 °C; for pyrolysis experiments, NH_3 slowly evaporated into the pyrolysis tube that contained a precursor in a quartz boat, and left the system through a bubbler. ^1H and $^{13}\text{C}\{^1\text{H}\}$ NMR spectra were recorded on a Varian Unity 400 at 25 °C from toluene- d_8 , benzene- d_6 , or hexane- d_{14} (with internal benzene- d_6) solutions and referenced vs. SiMe_4 by generally accepted methods; ^1H VT NMR data were obtained from 25 to 90 °C using a toluene- d_8 solution. Mass spectra were collected on a JEOL JMS-SX 102A spectrometer, EI mode, 20 eV. IR spectra of solids were acquired using KBr pellets on a BOMEM Michelson MB-100 FT-IR spectrometer. TGA/DTA were acquired under an UHP nitrogen flow, heating rate 5 °C/min, on a TA Instruments SDT 2960 simultaneous TGA/DTA apparatus. Elemental analyses were provided by E+R Microanalytical Laboratory, Corona, NY. Melting points (uncorrected) were determined with a Thomas-Hoover Uni-melt apparatus for samples flame-sealed in glass capillaries. Single-crystal X-ray diffraction study for $[\text{M}(\text{NMe}_2)_3]_2$, $\text{M} = \text{Al/Ga}$ (1/1), was performed at Clemson University, Clemson, SC, on a Nicolet R3m/V diffractometer using graphite-monochromated $\text{Mo K}\alpha$ radiation ($\lambda = 0.71073$ Å).¹⁰ All calculations were carried out using the SHELXTL suite of programs;¹¹ the structure was solved by direct methods. XRD data were collected using mineral oil coated samples on a Phillips XRD 3000 diffractometer utilizing $\text{Cu K}\alpha$ radiation; the average particle size, D , was calculated using the Scherrer equation¹² applied to low angle diffraction peaks. HRTEM microscopy (Topcon EM002B with 200 kV accelerating voltage) and energy dispersive spectroscopy, EDS (Topcon EM002B and Noran modem with an ultra thin window), were performed at the Analytical Instrumental Facility of North

Carolina State University, Raleigh. Room temperature photoluminescence (PL) data were recorded using a SPEX Fluorolog-2 instrument equipped with a double emission monochromator and a R928 photomultiplier tube. Excitation was provided by a 450 W Xe lamp whose output was focused into a 0.22 m monochromator to provide an excitation wavelength of 325 nm.

Preparation of the Al-amide-imide precursor. A sample of powdered $[\text{Al}(\text{NMe}_2)_3]_2$, 1.59 g (5.0 mmol), was placed in a 100 mL flask, and 30 mL of liquid NH_3 was condensed onto it at -78°C . The slurry was stirred at this temperature for two hours and then refluxed in liquid NH_3 for six hours. This was followed by a two-hour NH_3 boil-off yielding a white powdery solid, polymeric Al-amide-imide. The precursor was evacuated overnight. IR (cm^{-1}), broad bands: 680 (s), 802 (sh), 900 (s), 1018 (sh), 1262 (w), 1510 (w, sh), 1545 (m), 2775 (vw), 2857 (vw), 2927 (w), 2958 (w), 3200-3250 (w). EA (%): C, 5.89; H, 5.43; N, 37.59; H^*/N^* (i.e., excluding H and N in NMe_2), 1.62. TGA (weight loss): 30–250 $^\circ\text{C}$, 15%; 250–450 $^\circ\text{C}$, 5%.

Equilibration in the system $[\text{Al}(\text{NMe}_2)_3]_2/[\text{Ga}(\text{NMe}_2)_3]_2$ and formation of the mixed-metal compound $(\text{Me}_2\text{N})_2\text{Al}(\mu\text{-NMe}_2)_2\text{Ga}(\text{NMe}_2)_2$. Reference data (this study) for $[\text{Al}(\text{NMe}_2)_3]_2$: ^1H NMR: δ (toluene- d_8 /hexane- d_{14}) 2.34/2.50 (12H, $\mu\text{-NMe}_2$), 2.68/2.54 (24H, *exo*- NMe_2); $^{13}\text{C}\{^1\text{H}\}$ NMR: δ (toluene- d_8 /hexane- d_{14}) 42.0/41.5 (*exo*- NMe_2), 42.2/42.4 ($\mu\text{-NMe}_2$) and for $[\text{Ga}(\text{NMe}_2)_3]_2$: ^1H NMR: δ (toluene- d_8 /hexane- d_{14}) 2.47/2.62 (12H, $\mu\text{-NMe}_2$), 2.81/2.67 (24H, *exo*- NMe_2); $^{13}\text{C}\{^1\text{H}\}$ NMR: δ (toluene- d_8 /hexane- d_{14}) 44.0/43.5 (*exo*- NMe_2), 44.2/44.3 ($\mu\text{-NMe}_2$). For a 1/1 solution of $[\text{Al}(\text{NMe}_2)_3]_2$ (0.0318 g or 0.1 mmol) and $[\text{Ga}(\text{NMe}_2)_3]_2$ (0.0404 g or 0.1 mmol) in 0.7 mL of a solvent, three additional ^1H NMR peaks of equal integrated areas were seen at δ (toluene- d_8 /hexane- d_{14}) 2.40/2.55, 2.71/2.56, and 2.79/2.67 that were tentatively assigned, respectively, to the *exo*- $\text{Al}(\text{NMe}_2)_2$ (12H), $\text{Al}(\mu\text{-NMe}_2)_2\text{Ga}$ (12H), and *exo*-

$\text{Ga}(\text{NMe}_2)_2$ (12H) in the mixed-metal $[(\text{Me}_2\text{N})_2\text{Al}(\mu\text{-NMe}_2)_2\text{Ga}(\text{NMe}_2)_2]_2$. The $^{13}\text{C}\{^1\text{H}\}$ NMR peaks for this compound were at δ (toluene- d_8 /hexane- d_{14}) 41.9/41.4, 43.2/43.3, and 43.9/43.6. For a fresh toluene- d_8 solution of the 1/1 bimetallic mixture, room temperature ^1H NMR spectra were acquired at different times after preparation, the spectra were integrated, and expressed in terms of the percentage of the equilibration product in the solution: 15 minutes, < 1%; 2 h, 3%; 18 h, 28%, 48 h, 49%, 112 h, 53%. The remaining resonances were those of the distinct $[\text{Al}(\text{NMe}_2)_3]_2$ and $[\text{Ga}(\text{NMe}_2)_3]_2$ in an approximate 1/1 ratio. Similar results were obtained for parallel studies in benzene- d_6 and hexane- d_{14} . Another fresh toluene- d_8 solution of the 1/1 mixture was used in a ^1H VT NMR experiment which yielded the following contents of the equilibration product (in parentheses, holding time at a given temperature): 25 °C (1.5 h), 3%; 55 °C (10 min), 10%; 55 °C (0.5 h), 22%; 55 °C (1 h), 35%; 55 °C (2 h), 52%; 90 °C (0.5 h), 53%; cooled to 25 °C (1 h), 53%; 25 °C (24 h), 53%; the resonances for the remaining $[\text{Al}(\text{NMe}_2)_3]_2$ and $[\text{Ga}(\text{NMe}_2)_3]_2$ integrated in a 1/1 ratio. Suitable X-ray quality crystals¹⁰ were obtained at -30 °C from the fully equilibrated solution of $[\text{Al}(\text{NMe}_2)_3]_2$ and $[\text{Ga}(\text{NMe}_2)_3]_2$ in hexane (0.15 M each). Also, for crystalline solid: MS: m/e (intensity) (ion); clusters of peaks around: 359 (24) ($\text{AlGa}(\text{NMe}_2)_6 - \text{H}$ or $\text{M} - \text{H}$), 315 (47) ($\text{M} - \text{NMe}_2$), 273 (73) ($\text{M} - 2\text{NMe}_2 + \text{H}$; possible contribution from $\text{Al}_2(\text{NMe}_2)_5$), 228 (100) ($\text{M} - 3\text{NMe}_3$), 203 (8) ($\text{Al}(\text{NMe}_2)_4$; possible contribution from $\text{Ga}(\text{NMe}_2)_3$), 187 (6) ($\text{Ga}(\text{NMe}_2)_2(\text{NMe})$; possible contribution from $\text{Al}(\text{NMe}_2)_3(\text{NMe})$), 158 (12) ($\text{Ga}(\text{NMe}_2)_2 + \text{H}$; possible contribution from $\text{Al}(\text{NMe}_2)_3$), 115 (4) ($\text{Al}(\text{NMe}_2)_2$), 44 (6) (NMe_2). M.p., 89–91 °C.

Transamination in the bimetallic system $[\text{Al}(\text{NMe}_2)_3]_2/[\text{Ga}(\text{NMe}_2)_3]_2$, Al/Ga = 1/1. Preparation of precursor 1. Samples of $[\text{Ga}(\text{NMe}_2)_3]_2$, 2.02 g (5.0 mmol), and $[\text{Al}(\text{NMe}_2)_3]_2$, 1.59 g (5.0 mmol), were dissolved together in 30 mL of hexane and stirred at room temperature for 2 hours. This was equivalent to the formation of about 3% of the mixed-metal compound (see above). 30 mL of liquid NH_3 was transferred onto the

solution at $-78\text{ }^{\circ}\text{C}$ forming an immiscible liquid phase with hexane. The mixture was stirred at $-78\text{ }^{\circ}\text{C}$ for two hours which was followed by a two hour NH_3 boil-off at $-33\text{ }^{\circ}\text{C}$. The hexane slurry was then stirred overnight at room temperature, the volatiles removed, and the resulting white solid evacuated for two hours. EA (%): C, 10.82; H, 4.27; N, 24.78; H^*/N^* (i.e., excluding H and N in NMe_2), 1.16. IR (cm^{-1}), broad bands: 579 (s), 671 (s), 714 (s), 930 (m), 1513 (w, sh), 1544 (m), 2855 (vw), 2923 (w), 2960 (w, sh), 3200 (w).

Preparation of precursor 2. Samples of $[\text{Ga}(\text{NMe}_2)_3]_2$, 2.02 g (5.0 mmol), and $[\text{Al}(\text{NMe}_2)_3]_2$, 1.59 g (5.0 mmol), were dissolved together in 30 mL of pentane and stirred at room temperature for 14 hours. The volatiles were removed and a benzene- d_6 sample of the solid was prepared. Based on ^1H NMR, it contained about 20% of the mixed-metal compound. 30 mL of liquid NH_3 was deposited at $-78\text{ }^{\circ}\text{C}$ onto the isolated solid, the mixture stirred at this temperature for two hours, the NH_3 boiled off at $-33\text{ }^{\circ}\text{C}$ in two hours, and the solid product evacuated overnight. EA (%): C, 4.64; H, 3.95; N, 30.57; H^*/N^* (i.e., excluding H and N in NMe_2), 1.38. IR (cm^{-1}), broad bands: 575 (s), 690 (s), 720 (sh), 930 (s), 1250 (w), 1515 (sh), 1545 (m), 2857 (vw), 2955 (w), 3230 (w).

Preparation of precursor 3. Samples of $[\text{Ga}(\text{NMe}_2)_3]_2$, 2.02 g (5.0 mmol), and $[\text{Al}(\text{NMe}_2)_3]_2$, 1.59 g (5.0 mmol), were dissolved together in 30 mL of pentane and refluxed for three hours. The volatiles were removed and a benzene- d_6 sample of the solid was prepared. Based on ^1H NMR, it contained about 40% of the mixed-metal compound. 30 mL of liquid NH_3 was transferred at $-78\text{ }^{\circ}\text{C}$ onto the solid, the mixture refluxed in liquid NH_3 for six hours, volatiles removed, and the solid evacuated overnight. EA (%): C, 6.63; H, 3.68; N, 24.05; H^*/N^* (i.e., excluding H and N in NMe_2), 1.39. IR (cm^{-1}), broad bands: 575 (s), 675 (s), 929 (s), 1249 (w), 1380 (vw), 1515 (sh), 1545 (m), 2856 (vw), 2955 (w), 3200 (w). TGA (weight loss): 30–250 $^{\circ}\text{C}$, 5.9%; 250–450 $^{\circ}\text{C}$, 3.3%.

Preparation of precursor 4. Samples of $[\text{Ga}(\text{NMe}_2)_3]_2$, 2.02 g (5.0 mmol), and $[\text{Al}(\text{NMe}_2)_3]_2$, 1.59 g (5.0 mmol), were dissolved together in 30 mL of hexane and

refluxed for three hours. This was equivalent to about 53% of the mixed-metal compound in the solution. 30 mL of liquid NH_3 was transferred onto it at $-78\text{ }^\circ\text{C}$, the mixture refluxed in liquid NH_3 for six hours, volatiles removed, and the white product evacuated for two hours. EA (%): C, 2.73; H, 3.28; N, 29.33; H^*/N^* (i.e., excluding H and N in NMe_2), 1.29. IR (cm^{-1}), broad bands: 583 (s), 679 (s), 926 (s), 1246 (w), 1515 (sh), 1545 (m), 2928 (w), 2956 (w), 3190 (m). TGA (weight loss): 30–240 $^\circ\text{C}$, 5.1%; 250–450 $^\circ\text{C}$, 0.8%.

Pyrolysis studies. Bimetallic Al/Ga-amide-imide precursors 1–4 as well as the Al-amide-imide and Ga-imide^{4a} precursors were used in pyrolysis experiments. Preliminary pyrolyses under vacuum at 700 and 900 $^\circ\text{C}$ resulted in carbon containing black products and were discontinued. All subsequent experiments were performed under a flow of NH_3 at 700, 900, and 1100 $^\circ\text{C}$ for precursors loaded in a quartz boat. At pyrolysis temperatures of 900 $^\circ\text{C}$ and 1100 $^\circ\text{C}$ (especially), some corrosion of the boat's contact surface occurred (flaking) but the bulk product was apparently unaffected by interaction with silica. The most commonly used heating scheme consisted of pre-heating at 150 $^\circ\text{C}$ (1 h), ramping (15 minutes) to the final temperature at 700, 900, or 1100 $^\circ\text{C}$, and holding for three hours. Some samples, indicated with a pound sign (#) in sections a–c below, were also pyrolyzed using the following heating steps (in parentheses, holding time at given temperature): 150 $^\circ\text{C}$ (0.5 h), 400 $^\circ\text{C}$ (0.5 h), 600 $^\circ\text{C}$ (2 h), and final temperature at 700 or 900 $^\circ\text{C}$. The products were light colored, yellow to light gray, solids. They all were characterized by XRD spectroscopy, many by EA, IR, and PL methods, and selected ones by TEM/EDS techniques.

(a) Pyrolysis of Ga-imide to afford GaN. 700 $^\circ\text{C}$, yellow; XRD, cubic/hexagonal GaN ($D = 5\text{ nm}$). 700 $^\circ\text{C}$,[#] yellow; XRD, cubic/hexagonal GaN ($D = 6\text{ nm}$). 900 $^\circ\text{C}$,[#] yellow; XRD, hexagonal GaN ($D = 21\text{ nm}$). 1100 $^\circ\text{C}$, yellow; IR (cm^{-1}): 580 (br); XRD, hexagonal GaN ($D = 23\text{ nm}$).

(b) Pyrolysis of Al-amide-imide to afford AlN. 900 °C, light gray; XRD, hexagonal AlN ($D = 5$ nm). 1100 °C, light gray; EA (%) found (calcd for AlN): N, 33.78 (34.17); C, < 0.3 (0); H, < 0.1 (0); IR (cm^{-1}): 680 (br); XRD, hexagonal AlN ($D = 10$ nm).

(c) Pyrolysis of Al/Ga-amide-imide precursors 1–4 to afford composites. In the XRD diffractograms of some of the materials pyrolyzed at 1100 °C, two partially overlapped hexagonal patterns are discernible: one with sharp, high intensity peaks (GaN-type) and the second with very broad, much less intense peaks (AlN-type). In one favorable case, two calculated average particle sizes, $D(\text{sharp})/D(\text{broad})$, D_s/D_b , are included (*vide infra*). Precursor 1: 700 °C, gray; IR (cm^{-1}): 700 (br); XRD, cubic/hexagonal ($D = 4$ nm). 700 °C,[#] gray; EA (%) found (calcd for AlGa₃N₂): N, 22.18 (22.46); C, 0.73 (0); H, 0.34 (0); XRD, cubic/hexagonal ($D = 5$ nm). 900 °C, light gray; EA (%) found (calcd for AlGa₃N₂): N, 20.29 (22.46); C, 0.21 (0); H, 0.16 (0); XRD, hexagonal ($D = 13$ nm). 900 °C,[#] light gray; EA (%) found (calcd for AlGa₃N₂): Ga, 52.57 (55.90); Al, 21.98 (21.63); N, 20.42 (22.46); C, 0.25 (0); H, 0.20 (0); Al/Ga = 1.08; XRD, hexagonal ($D = 15$ nm). 1100 °C, light gray; IR (cm^{-1}): 675 (br), 600 (sh); XRD, hexagonal ($D = 18$ nm). Precursor 2: 900 °C, light gray; IR (cm^{-1}): 675 (br), 600 (sh); XRD, hexagonal ($D = 20$ nm). 1100 °C, light gray; XRD, hexagonal ($D = 23$ nm). Precursor 3: 900 °C, light gray; IR (cm^{-1}): 670 (br), 590 (sh); XRD, hexagonal ($D = 18$ nm). 1100 °C, light gray; EA (%) found (calcd for AlGa₃N₂): N, 21.95 (22.46); C, < 0.1 (0); H, < 0.1 (0); IR (cm^{-1}): 670 (br), 615 (sh); XRD, hexagonal ($D = 20$ nm). Precursor 4: 700 °C, light gray; EA (%) found (calcd for AlGa₃N₂): N, 22.19 (22.46); C, 0.33 (0); H, 0.24 (0); IR (cm^{-1}), broad bands: 3225 (w), 2168 (w), 920 (w), 679 (s), 594 (s); XRD, cubic/hexagonal ($D = 6$ nm). 900 °C, light gray; IR (cm^{-1}), broad bands: 675 (s); 595 (s); XRD, hexagonal ($D = 13$ nm). 1100 °C, light gray; EA (%) found (calcd for AlGa₃N₂): N, 20.17 (22.46); C, 0.20 (0); H, 0.10 (0); IR (cm^{-1}): 675 (br), 600 (sh); XRD, hexagonal ($D_s/D_b = 15\text{nm}/8\text{nm}$).

Results and Discussion

Nanocrystalline AlN *via* transamination/deamination of $[\text{Al}(\text{NMe}_2)_3]_2$

The reactions between $[\text{Al}(\text{NMe}_2)_3]_2$ and liquid NH_3 resulted in an advantageous precursor whose chemical make-up was consistent with the polymeric Al-amide-imide, $[\text{Al}(\text{NH}_2)(\text{NH})]_n$, containing some residual NMe_2 groups (equation 1). The EA data yielded the H/N ratio of 1.62 (excluding NMe_2 groups estimated from the C content) vs. 1.50 for the Al-amide-imide. IR spectroscopy also provided strong structural evidence by displaying, in addition to weak NMe_2 -associated bands, a signature band at 1545 cm^{-1} (NH_2) with the distinct shoulder at 1515 cm^{-1} (NH) for the NH_2/NH groupings in $[\text{Al}(\text{NH}_2)(\text{NH})]_n$.^{6b} The number of residual NMe_2 groups could be estimated from the EA data and amounted to about one such group per eight aluminum atoms. The total TGA weight loss of 20% for the material was lower than the calculated 29.4% for the Al-amide-imide: continued deamination in the fresh precursor could be partly responsible for the discrepancy.

The pyrolysis of the Al-amide-imide was initially carried out under vacuum and resulted in a black solid that was shown by XRD spectroscopy to be hexagonal AlN. The black tinge indicated a high level of carbon retained in the product. The pyrolysis of the Al-amide-imide to light gray, nanocrystalline AlN was successfully performed at 900 and 1100 °C under NH_3 flow, a treatment which is known to substantially remove NR_2 -carbons as HNR_2 and improve the product's crystallinity.¹³ A partial elemental analysis was done for the latter material and showed a satisfactory N content, and the C and H contents below detection limits of applied analytical procedures, consistent with high purity AlN. The IR broad band at 680 cm^{-1} was typical for AlN. The products were shown by XRD to be hexagonal. 2H-wurtzite AlN (JCPDS file 25-1133; reported: $a = 3.111\text{ \AA}$, $c = 4.979\text{ \AA}$). Due to the broadness of the pattern, accurate calculations of "a" and "c" were not attempted.

Approximate determinations were done, however, using Bragg's equation and the (002) diffraction for "c" and (110) diffraction for "a"; the estimated values were $a = 3.11 \text{ \AA}$ and $c = 4.96 \text{ \AA}$, and agreed satisfactorily with those reported for AlN. The crystallite sizes averaged 5 nm (900 °C) and 10 nm (1100 °C).

Equilibration in the system $[\text{Al}(\text{NMe}_2)_3]_2/[\text{Ga}(\text{NMe}_2)_3]_2$, Al/Ga = 1/1

The encouraging results for the separate transaminations of $[\text{Al}(\text{NMe}_2)_3]_2$ and $[\text{Ga}(\text{NMe}_2)_3]_2$ ^{4a} prompted us to look into the mixed system composed of these two compounds. We first studied possible exchange processes taking place in toluene, benzene, or hexane solutions containing equimolar quantities of the compounds as the means to pre-forming the Al-N(Me₂)-Ga bridges. Indeed, we discovered that the solutions were involved in exchanges leading to the formation of the homoleptic four-membered ring compound $(\text{Me}_2\text{N})_2\text{Al}(\mu\text{-NMe}_2)_2\text{Ga}(\text{NMe}_2)_2$ in admixture with separate $[\text{Al}(\text{NMe}_2)_3]_2$ and $[\text{Ga}(\text{NMe}_2)_3]_2$, stable on the NMR time scale (*vide infra*, Scheme 1). For example, a typical ¹H NMR spectrum in toluene-d₈ showed, in addition to the resonances for the distinct parent dimers, three new peaks at δ 2.40, 2.71, and 2.79 that grew with time, and which were tentatively assigned, based on comparison with the signals for the parent dimers, respectively, to the *exo*-Al(NMe₂)₂, Al(μ -NMe₂)₂Ga, and *exo*-Ga(NMe₂)₂ protons in the equilibration product $(\text{Me}_2\text{N})_2\text{Al}(\mu\text{-NMe}_2)_2\text{Ga}(\text{NMe}_2)_2$. Some support for the existence of the mixed-metal compound also in the solid state came from the mass spectrum obtained for the crystalline equilibration product. The highest m/e cluster of peaks in the spectrum was found at m/e 359, i.e., one unit smaller than the parent ion for the mixed-metal compound at m/e 360.

The solution system appeared to reach equilibrium at about 53% content of the mixed-metal compound and equimolar quantities of the separate initial dimers after a few days at room temperature. On the other hand, a similar equilibrium level was reached after

only two hours if the fresh toluene solution was heated to 55 °C. Once reached, this level seemed to remain stable within the accuracy of our determinations in the temperature range from 25 to 90 °C or in the course of several days at room temperature. The solid that crystallized from the equilibrated solution, which was subsequently redissolved in benzene- d_6 , was shown by NMR spectroscopy to consist of the same equilibrated species as seen before crystallization, i.e., about 53% of mixed-metal $(Me_2N)_2Al(\mu-NMe_2)_2Ga(NMe_2)_2$ and equimolar $[Al(NMe_2)_3]_2$ and $[Ga(NMe_2)_3]_2$.

An X-ray single-crystal structure determination was attempted for the solid that crystallized in this bimetallic system in order to further address the question of equilibration products. The obtained structure features a planar four-membered ring with the $\{M-N-M-N\}$ core.¹⁰ This compares well with the structures known for the parent dimers $[Al(NMe_2)_3]_2$ ^{9b, 14} and $[Ga(NMe_2)_3]_2$.^{9b} The centrosymmetric space group of the crystallographic solution requires that the unique metal site M represents a 50% occupation by both Al and Ga atoms. In general, such a structural solution could originate either from the $\{Al-N-Ga-N\}$ alternating cores in packing stacks, or from intimately cocrystallized separate dimers $Al(NMe_2)_3$ and $[Ga(NMe_2)_3]_2$, or from both the cocrystallized separate dimers and mixed-metal compound. Regardless of the intrinsic limitations in the interpretation of the structural data, they are consistent with an efficient mixing of the species on the molecular level.

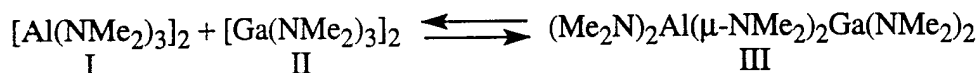
Aluminum/gallium nitride nanocomposites *via* transamination/deamination in the system $[M(NMe_2)_3]_2/NH_3$, M = Al/Ga (1/1).

Transamination/deamination in the system $[M(NMe_2)_3]_2/NH_3$, M = Al/Ga (1/1), was performed for the reactants pre-equilibrated in hexane or pentane at various levels, i.e., 3%, 20%, 40%, and 53% of the mixed-metal compound. They were either isolated as solids by evacuation of the solvent (20% and 40% cases) or remained in the solution (3%

and 53% cases) for reaction with liquid NH₃. Following the condensation of NH₃ at -78 °C, the system was warmed to about -33 °C, at which point NH₃ was refluxed and/or allowed to slowly boil-off. This was followed by evacuation at room temperature and resulted in precursors 1–4 as summarized in Scheme 1.

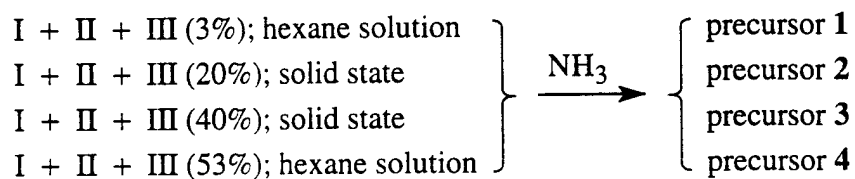
Scheme 1

1. Equilibration in hexane solution:



2. Reactions of equimolar I and II and varying amounts of III with NH₃:

(I + II + III = 100%)



All four precursors contained abundant NH₂/NH groups and small quantities of residual NMe₂ groups, as inferred from the EA and IR data. For reference purposes below, a 1:1 mixture of [Al(NH₂)(NH)]_n (H/N, 1.50) and [Ga (NH)_{3/2}]_n (H/N, 1.00) would show H/N at about 1.29. Precursor 1 (3% case) had the C content of 10.82% and H*/N* (i.e., excluding H and N in NMe₂) ratio of 1.16. This could be compared with precursor 4 (53% case) showing the C content of 2.73% and H*/N* ratio equal to 1.29, a striking match with the reference value above. The precursors obtained from the reactions between NH₃ and isolated solids, 2 (20% case) and 3 (40% case), showed these values at: C, 4.64; H*/N*, 1.38 and C, 6.63; H*/N*, 1.39, respectively. It would seem that precursor 4 was the most deeply converted towards Al/Ga-amide-imide. All these precursors might be envisioned as having some proportion of mixed crosslinking resulting, for instance, from transamination [Al–N(Me₂)–Ga + NH₃ = Al–N(H₂)–Ga + HNMe₂] or deamination [Al–NMe₂ + H₂N–Ga = Al–N(H)–Ga + HNMe₂]. The extent of it, in the

first approximation, could perhaps be related to the progress of equilibration in the bimetallic system $[\text{Al}(\text{NMe}_2)_3]_2/[\text{Ga}(\text{NMe}_2)_3]_2$ via formation of the mixed Al-N(Me₂)-Ga linkages.

The precursors were pyrolyzed under a NH_3 flow, independently at 700 (some precursors), 900, and 1100 °C resulting in light gray composites. These temperature limits were set as a compromise between efficient conversion/crystallization rates and thermal stabilities of the nitrides. Despite some inconsistencies in the literature,¹⁵ AlN appears be stable even at 1700 °C while GaN apparently decomposes above 1000–1100 °C. Higher temperatures than 700 °C should have promoted the formation of hexagonal GaN as opposed to the preferred cubic/hexagonal variety observed at lower temperatures,^{4, 16} and this could be beneficial for alloying with hexagonal AlN. The products showed very low residual C and H contents, and N contents in the 20.17–22.19% range, close to the expected value for the AlGa_2N_3 composition, 22.46%. The IR spectra for the products (900 and 1100 °C) were quite similar displaying one broad band centered at 670–680 cm^{-1} (Al–N stretch) with a distinct shoulder at 580–600 cm^{-1} (Ga–N stretch).

The reference XRD patterns obtained in this study for pure nitrides (Figure 1) and for an approximately 1:1 physical mixture of AlN and GaN (Figure 2C) illustrate the general appearance of the diffractograms; note, the much less intense patterns for AlN, a result of the pronounced peak broadness associated with the materials' extreme nanocrystallinity. The XRD patterns were also obtained for all composites and, generally, they displayed two distinct characteristics depending on pyrolysis temperature. For materials heated at 700 °C, the patterns were consistent with a nanocrystalline, cubic/hexagonal phase of GaN as previously observed for pyrolysis of the Ga-imide⁴ or by comparison with pure GaN from pyrolysis at 700 °C in this study (Figure 1A). On the other hand, samples pyrolyzed at 900 and 1100 °C showed a rather sharp, strong hexagonal pattern of the GaN type (improved for 1100 °C) but also a second, much broader

and less intense, frequently superimposed hexagonal pattern that appeared to be derived from the AlN lattice.

This is illustrated in Figure 2 where three XRD patterns, all related to the pyrolysis of different precursors at 1100 °C, are included. The figure on the right shows the expansions of the 2θ 30–40° region. It is clear that the GaN-type pattern (sharp lines) is severely superimposed over the AlN-type pattern (broad lines). For example, in spectrum B for precursor 1, a severe overlap of the two types of patterns takes place and results in broadening of the sharp peaks' bases beyond distinct separation. The AlN-type component in spectrum A is not pure AlN because it shows different peak positions than those for the AlN reference. Figure 3 shows the XRD patterns for the composites obtained from precursor 4 at 700, 900, and 1100 °C, and illustrates the temperature related effect on the patterns.

Table 1 summarizes the average crystallite sizes and rough estimates of lattice parameters, whenever possible, and the latter were done using Bragg's equation and the (002) diffraction for "c" and (110) diffraction for "a", as discussed earlier for pure AlN. For example, for precursor 4, the biggest change in the average crystallite size for the GaN-type component is noticed when going from 700 °C (not shown in table), 6 nm, to 900 °C, 13 nm, and much smaller change to 1100 °C, 15 nm. The comparison of the lattice parameters for the GaN-type with those for pure GaN shows that they approach each other, especially for composites pyrolyzed at 1100 °C. Regarding the second identified component, AlN-type lattice, both "a" and "c" constants are close to the average values for pure AlN and pure GaN, which, according to the Vegard's law, indicates an AlGa₂N solid solution with equal proportions of Al and Ga. This can be compared with the report, not detailed though, on the bulk solid solutions of AlN and GaN,^{15a} in which the 1:1 solution is quoted to have the GaN type of hexagonal lattice. It is also interesting to note that, based strictly on mass balance considerations, the presence of pure GaN (GaN-type) with the concurrent 1:1 Al/Ga solid solution (AlN-type) requires a third, aluminum rich phase,

possibly pure AlN. This nanophase in small quantities would not be easily seen by XRD due to its extreme peak broadness and overlap with the major spectral components. In summary, the XRD data suggest that there are two to three distinct hexagonal phases in these composites that differ quite significantly in their average particle sizes and compositions.

TEM/EDS measurements were undertaken in order to probe the composites from another angle. Figures 4 and 5 show typical grain habit/crystallinity and electron diffraction patterns. In general, the samples pyrolyzed at 700 °C (for example, Figure 4A) are composed of quite uniformly sized particles with diameters less than several nanometers. They are crystalline and the electron diffraction patterns show rather diffuse lines with infrequent spots consistent with basic nanocrystalline character. The EDS data for the material shown in Figure 4A, provide the relative Ga contents of 52–55% and Al contents of 45–48%. These estimates are consistent with equimolar Al/Ga ratios homogeneously distributed in the material. On the other hand, the samples prepared at 900 and 1100 °C are similar to each other, and display an apparent bimodal size distribution. They show a fraction of very large crystallites, bigger than 80–100 nm, which are usually embedded in a matrix of particles smaller than 20–30 nm (for example, Figure 4B, left, and Figure 5, top). The electron diffraction patterns for the biggest particles from the pyrolysis at 1100 °C confirm their single crystal nature (Figure 5, bottom, right) and EDS gives the relative Ga contents higher than 95%, and this may simply correspond to pure GaN. The electron diffraction pattern for the matrix particles in this material (Figure 5, bottom, left) shows the spotty rings reflecting polycrystallinity and particles bigger than several nanometers. The EDS data for the matrix in this sample provide the relative Ga contents of 28–31% and Al contents of 69–72%, i.e., material on average enriched in aluminum. Very similar EDS results to those discussed above were also obtained for both the large crystallites and finer particles in the composite from precursor 1 pyrolyzed at 900 °C. These averaged EDS results for the matrix can be interpreted as describing a mixture of

homogeneously dispersed two separate phases suggested earlier from the XRD data and mass balance considerations, i.e., one phase of the AlGa₂N solid solution with the Al/Ga ratio close to 1/1, and the postulated second phase of possibly pure AlN.

Some preliminary room temperature photoluminescence (PL) measurements of the composites have been carried out employing an excitation wavelength of 325 nm, a value commonly used to excite the luminescence of homogeneous GaN materials (a bulk E_g of around 3.4 eV). The Xe lamp employed in our PL spectrometer does not possess sufficient power in the far UV region necessary to excite the bulk bandgap of AlN (6.2 eV) or any corresponding possible Al-rich nitride phases. As a consequence, the focus of these measurements is limited to an examination of gallium-rich nitride phases or pure GaN domains, if any. For a given pyrolysis temperature (for example, 900 °C), the composites from precursors 1–3 show similar PL spectra which are in stark contrast with the emission observed for the composites from precursor 4. In the case of the nitride derived from pyrolysis of precursor 1 at 900 °C (Figure 6A), very broad emission centered around 550 nm is observed. While yellow-green defect PL in this type of sample apparently dominates the photophysics, one cannot rule out some contribution of weak band edge blue PL based on the substantial linewidth (FWHM, about 250 nm) of this emission. This conclusion is supported by the fact that pyrolysis of this same precursor at 1100 °C results in the shift in the defect feature to longer wavelength, making the detection of a distinct shoulder in the blue region more facile. Both these PL features have been previously observed and their origin discussed for bulk nanophase GaN^{4b, c} as well as in epitaxial thin films.¹⁷ In contrast, spectra obtained for the composite from precursor 4 pyrolyzed at 900 °C (Figure 6B) show very strong blue emission at approximately 420 nm and a negligible yellow component. For these samples, there is a positive correlation between the relative intensity of the yellow emission and the pyrolysis temperature employed to convert the precursor to the nitride composite, with the most intense defect emission observed in samples pyrolyzed at 1100 °C. This data may be indicative of thermally generated lattice defects at

temperatures approaching the reported thermal stability limits for GaN (1000–1100 °C). There are some differences in the relative intensities of the emission maxima among the composites but no clear correlation is apparent from the data presented. In summary, the PL measurements are consistent with the presence of the GaN component in these composites which we believe corresponds to the GaN-type phase earlier emerging from the XRD and TEM/EDS data. We plan extended photoluminescence studies employing shorter excitation wavelengths which, coupled with Raman spectroscopy, will elucidate the character of other components of the composites.

The materials characterization results can be reconciled with the following nature of the synthesized nitride composites. First, the composites obtained at 700 °C seem to be prevailingly cubic/hexagonal nanolattices of the known phase-inhomogeneous GaN; no other distinct phases were detected on the several nanometer scale. These materials also appear to be chemically homogeneous on this scale. However, it is possible that there is some chemical and phase inhomogeneity on the smaller than a few nanometer scale which we were unable to probe. It is thus probable that the postulated second AlN-type component, possibly pure AlN, which may be emerging from the precursors' pyrolysis at this temperature, is still not completely converted and of extremely small particle sizes. This is a viable supposition since for the Al-amide-imide precursor pyrolyzed at 900 °C the average particle size is only 5 nm and much smaller sizes would be expected at 700 °C. Such a structural make-up of the 700 °C composites could have escaped differentiation by XRD, EDS, and even standard HRTEM techniques. On the other hand, the composites obtained at 900 and 1100 °C have much in common and the latter temperature is in their upper stability limits. These materials appear to be composed of, at least, two detected crystallographic hexagonal phases, pure GaN and AlGa₂N solid solution with Al/Ga approximately 1/1, and, postulated pure AlN. The particles made of these phases form an apparent multimodal size distribution system. The smallest particles contain a mixture of

pure AlN and AlGa₂N solid solution while the largest particles appear to be pure GaN; some particles of the latter phase are very large reaching more than 100 nm.

The picture emerging from the results and discussion above is consistent with the existence of correlation between the chemical nature of the starting bimetallic Al/Ga-amide-imide precursors and the resulting make-up of the composites derived from them. The presence in an initial reaction mixture of three different species with distinct bonding situations, Ga–N(Me₂)–Ga, Al–N(Me₂)–Al, and mixed-metal Ga–N(Me₂)–Al, seems to lead upon transamination/deamination with NH₃ to a precursor preserving these three bonding domains, now, *via* transaminated nitrogen bridges. The following pyrolysis leads to elimination-condensation, to a large degree, separately within these three domains, and formation at appropriate temperatures of three distinct hexagonal phases evolved from them. These phases are consistent with AlN, GaN, and AlGa₂N (Al/Ga = 1/1) solid solution of aluminum/gallium nitride, and directly reflect the chemical make-up of the precursor. We were, unfortunately, unable to confirm any clear quantitative trend among the different precursors in relation to the nature of the resulting composites. This is mainly due to inherent problems to quantify the results of the characterization methods which we used. We notice, however, that the most intense peaks of the AlN-type (AlGa₂N solid solution) in the XRD spectra are obtained for the composites derived from precursors **3** and **4**, but not **1**, i.e., for those containing significant mixed Al–N–Ga bridges, in qualitative agreement with the above. Further efforts are underway to address the quantitative aspect of composite formation as well as perform composites' extended characterization by photoluminescence at lower excitation wavelengths and by Raman spectroscopy.

Note Added in Proof. Since submission of this paper, a report on the proposed cubic AlGa₂N solid solution/polymer composite formation at 600 °C from a similar reaction system has been published.¹⁸ Our paper appears to be complementary in that it addresses the chemical aspects of precursor formation and nature as well as deals with conversion

temperatures higher than 600 °C. At the same time, it is somewhat controversial since we are reporting rather complex hexagonal aluminum/gallium nitride composites obtained under these conditions.

Acknowledgment. R. L. Wells wishes to thank the Office of Naval Research for its financial support. J. L. Coffey thanks the Robert A. Welch Foundation for support. We also want to thank Dr. Serge Oktriabrsky from the North Carolina State University for his help in evaluating the TEM/EDS results.

Supporting Information Available: Thermal ellipsoid diagram, tables of bond distance and angles, anisotropic displacement coefficients, atomic fractional coordinates and U values, and observed and calculated structure factors for $[M(NMe_2)_3]_2$, $M = Al/Ga(1/1)$. Ordering information is given on any current masthead page.

References

- (1) For example, see (and references therein): (a) Paine, R. T. *J. Inorg. Organometal. Polymers* **1992**, 2, 183. (b) Sauls, F. C.; Interrante, L. V. *Coord. Chem. Reviews* **1993**, 128, 193. (c) Sheppard, L. M. *Am. Cer. Soc. Bull.* **1990**, 69, 1801. (d) Baker, R. T.; Bolt, J. D.; Reddy, G. S.; Roe, D. C.; Staley, R. H.; Tebbe, F. N.; Vega, A. J. *Mater. Res. Soc. Symp. Proc.* **1988**, 121, 471.
- (2) For example, see reviews: (a) Nakamura, S. *Mater. Science Eng.* **1997**, B43, 258. (b) Morkoç, H. *Mater. Science Eng.* **1997**, B43, 137. (c) Akasaki, I.; Amano, H. *J. Cryst. Growth* **1997**, 175/176, 29.
- (3) (a) Paine, R. T.; Janik, J. F.; Fan, M. *Polyhedron*, **1994**, 13, 1225 and references therein. (b) Kwon, D.; Schmidt, W. R.; Interrante, L. V.; Marchetti, P.; Maciel, G. in *Inorganic and Organometallic Oligomers and Polymers*; Harrod, J. F. and Laine, R. M., Eds: Kluwer Academic, Hingham, MA, U.S.A., **1991**, 191. (c) Mazdiasni, K. S.; Ruh, R.; Hermes, E. E. *Am. Ceram. Soc. Bull.* **1985**, 64, 1149. (d) Twait, D. J.; Lackey, W. J.; Smith, A. W.; Lee, W. Y.; Hanigofsky, J. A. *J. Am. Ceram. Soc.* **1990**, 73, 1510.
- (4) (a) Janik, J. F.; Wells, R. L. *Chem. Mater.* **1996**, 8, 2708. (b) Wells, R. L.; Janik, J. F.; Gladfelter, W. L.; Coffey, J. L.; Johnson, M. A.; Steffey, B. D. *Mater. Res. Soc. Symp. Proc.* **1997**, 468, 39. (c) Coffey, J. L.; Johnson, M. A.; Zhang, L.; Wells, R. L.; Janik, J. F. *Chem. Mater.* **1997**, 9, 2671. (d) Wells, R. L.; Gladfelter, W. L. *J. Cluster Science* **1997**, 8, 217.
- (5) (a) Hoffman D. M. *Polyhedron* **1994**, 8, 1169. (b) Gordon, R. G.; Hoffman, D. M.; Riaz, U. *Mater. Res. Soc. Symp. Proc.* **1991**, 204, 95. (c) Gordon, R. G.; Hoffman, D.

M.; Riaz, U. *Chem. Mater.* **1990**, *2*, 480. (d) Riaz, U.; Gordon, R. G.; Hoffman, D. M. *Chem. Mater.* **1992**, *4*, 68.

(6) (a) Wiberg, E.; May, A. *Z. Naturforsch.* **1955**, *10b*, 229. (b) Maya, L. *Adv. Ceram. Mater.* **1986**, *1*, 150. (c) Maya, L. *Inorg. Chem.* **1992**, *31*, 1958.

(7) (a) Hagen, J.; Metcalfe, R. D.; Wickenden, D.; Clark, W. *J. Phys. C: Solid State Phys.* **1978**, *11*, L143. (b) Baranov, B.; Däveritz, L.; Gutan, V. B.; Jungk, G.; Neumann, H.; Raidt, H. *Phys. Stat. Sol. (a)* **1978**, *49*, 629. (c) Angerer, H.; Ambacher, O.; Stutzmann, M.; Metzger, T.; Höpler, R.; Born, E.; Bergmaier, A.; Dollinger, G. *Mater. Res. Soc. Symp. Proc.* **1997**, *468*, 305. (d) Leitner, J. *J. Phys. Chem. Solids* **1997**, *58*, 1329.

(8) Osamura, K.; Naka, S.; Murakami, Y. *J. Appl. Phys.* **1975**, *46*, 3432.

(9) (a) Nöth, H.; Konrad, P. *Z. Naturforsch.* **1975**, *30b*, 681. (b) Waggoner, K. M.; Olmstead, M. M.; Power, P. P. *Polyhedron* **1990**, *9*, 257.

(10) Crystallographic data for planar dimer $[M(NMe_2)_3]_2$, $M = Al/Ga(1/1)$ (295 K): $C_{12}H_{36}N_6AlGa$, MW = 361.17, triclinic, space group P1(No. 2), $a = 7.485(3) \text{ \AA}$, $b = 8.668(3) \text{ \AA}$, $c = 8.879(3) \text{ \AA}$, $\alpha = 60.64(2)^\circ$, $\beta = 84.55(3)^\circ$, $\gamma = 88.11(3)^\circ$, $V = 499.8(3) \text{ \AA}^3$, $F(000) = 194$, $Z = 1$, $D_c = 1.200 \text{ g/cm}^3$, $\mu = 14.2 \text{ cm}^{-1}$, specimen size (mm) $0.30 \times 0.40 \times 0.50$, 1512 reflections collected, 1389 unique reflections ($R_{int} = 0.0201$), 2θ range for data collection, $3.5\text{--}46.0^\circ$, scan type $\omega/2\theta$. All non-hydrogen atoms were refined anisotropically. Due to the high thermal motion of the methyl carbon atoms, hydrogen atoms were not included. The final cycle of full-matrix least-squares refinement was based on 1126 observed reflections ($I > 2\sigma(I)$) and 91 variable parameters and converged (largest

parameter shift was 0.0022 times its esd) with final residual values of $R = 0.0532$, $R_w = 0.0689$, and $S = 1.97$. Refinement in the noncentrosymmetric space group, $P1$, resulted in a disordered model that was experimentally equivalent to the structure obtained in $P-1$. Selected distances (Å): $M-(\mu-N)$, 2.002 (av); $M-(exo-N)$, 1.828(8); $N-C$, 1.48 (av). Ring angle: $M-(\mu-N)-M$, 91.5° . Thermal ellipsoid diagram, bond distances and angles, and acquisition parameters are included in Supporting Information.

(11) (a) Sheldrick, G. M. *SHELXTL, Crystallographic Computing System*, Nicolet Instruments Division: Madison, WI, 1986. (b) *International Tables for X-ray Crystallography*, The Kynoch Press, Birmingham, England, 1974.

(12) Klug, P. H.; Alexander, E. L.; in *X-Ray Diffraction Procedures*, John Wiley & Sons, Inc., New York (1974), p. 656 and references therein.

(13) For example, see: (a) Sauls, F. C.; Hurley, W. J.; Interrante, L. V.; Marchetti, P. S.; Maciel, G. E. *Chem. Mater.* **1995**, 7, 1361. (b) Paine R. T., in *Inorganometallic Chemistry* (Fehlner, T. P., Ed.), Plenum Press, New York (1992), p. 359 and references therein. (c) Koyama, S.; Takeda, H.; Saito, Y.; Sugahara, Y.; Kuroda, K. *J. Mater. Chem.* **1996**, 6, 1055.

(14) Ouzounis, K; Riffel, H; Hess, H; Kohler, U; Weidlein, J. Z. *Anorg. Allg. Chemie* **1983**, 504, 67.

(15) (a) Lyutaya, M. D.; Bartnitskaya, T. S. *Inorg. Mater. (Izvestiya Akademii Nauk SSSR, Neorganicheskie Materialy)* **1973**, 9(7), 1052 (Russian version, p.1186). (b) Neumayer, D. A.; Ekerdt, J. G. *Chem. Mater.* **1996**, 8, 9 and references therein.

(16) Hwang, J.-W.; Campbell, J. P.; Kozubowski, J.; Hanson, S. A.; Evans, J. F.; Gladfelter, W. L. *Chem. Mat.* **1995**, *7*, 517.

(17) (a) Ogino, T.; Aoki, M. *Jpn. J. Appl. Phys.* **1980**, *19*, 2395. (b) Hofman, D. M.; Kovalev, D.; Steude, G.; Meyer, B. K.; Hoffman, A.; Eckey, L.; Detchprom, T.; Amano, H.; Akasaki, I. *Phys. Rev. B* **1995**, *52*, 16702. (c) Glaser, E.; Kennedy, T.; Doverspike, K.; Rowland, L.; Gaskill, D.; Freitas, J.; Asif Khan, M.; Olson, D.; Kuznia, J.; Wickenden, D. *Phys. Rev. B* **1995**, *51*, 13326.

(18) Benaissa, M.; Gonsalves, K. E.; Rangarajan, S. P. *Appl. Phys. Lett.* **1997**, *71*, 3685.

Table 1. Average particle sizes (D) and estimated lattice parameters (a, c) derived from XRD patterns for hexagonal phases in composites and pure nitrides.

	900 °C						1100 °C					
	composite from precursor				GaN	AlN	composite from precursor				GaN	AlN
	1	2	3	4			1	2	3	4		
average size, D (nm)	13	20	18	13	21	5	18	23	20	15/8	23	10
GaN-type, a (Å)	3.16	3.18	3.18	3.17	3.19		3.18	3.18	3.18	3.17	3.18	
c (Å)	5.13	5.16	5.14	5.12	5.19		5.16	5.15	5.15	5.16	5.17	
AlN-type, a (Å)	-	3.15	3.14	3.14		3.09	3.15	3.14	3.13	3.13		3.11
c (Å)	-	-	-	5.05		4.93	5.09	5.05	5.06	5.06		4.96

Figure captions

Figure 1. XRD patterns for pure nitrides, GaN and AlN, obtained, respectively, from gallium imide and aluminum amide imide at different temperatures: (A) GaN, 700 °C; (B) GaN, 900 °C; (C) GaN, 1100 °C; (D) AlN, 1100 °C.

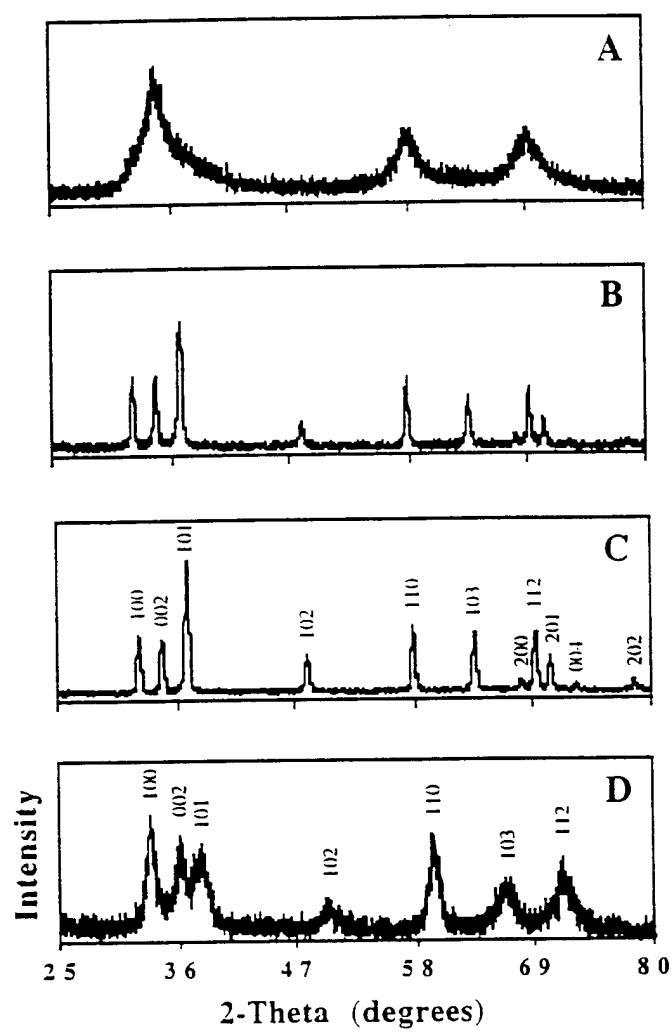
Figure 2. XRD patterns for precursors pyrolyzed at 1100 °C; right side, expansion of the 2θ 30–40 ° region: (A) composite from precursor 4 (AlGa₂N stands for aluminum/gallium nitride solid solution phase); (B) composite from precursor 1; (C) AlN/GaN, 1/1 physical mixture.

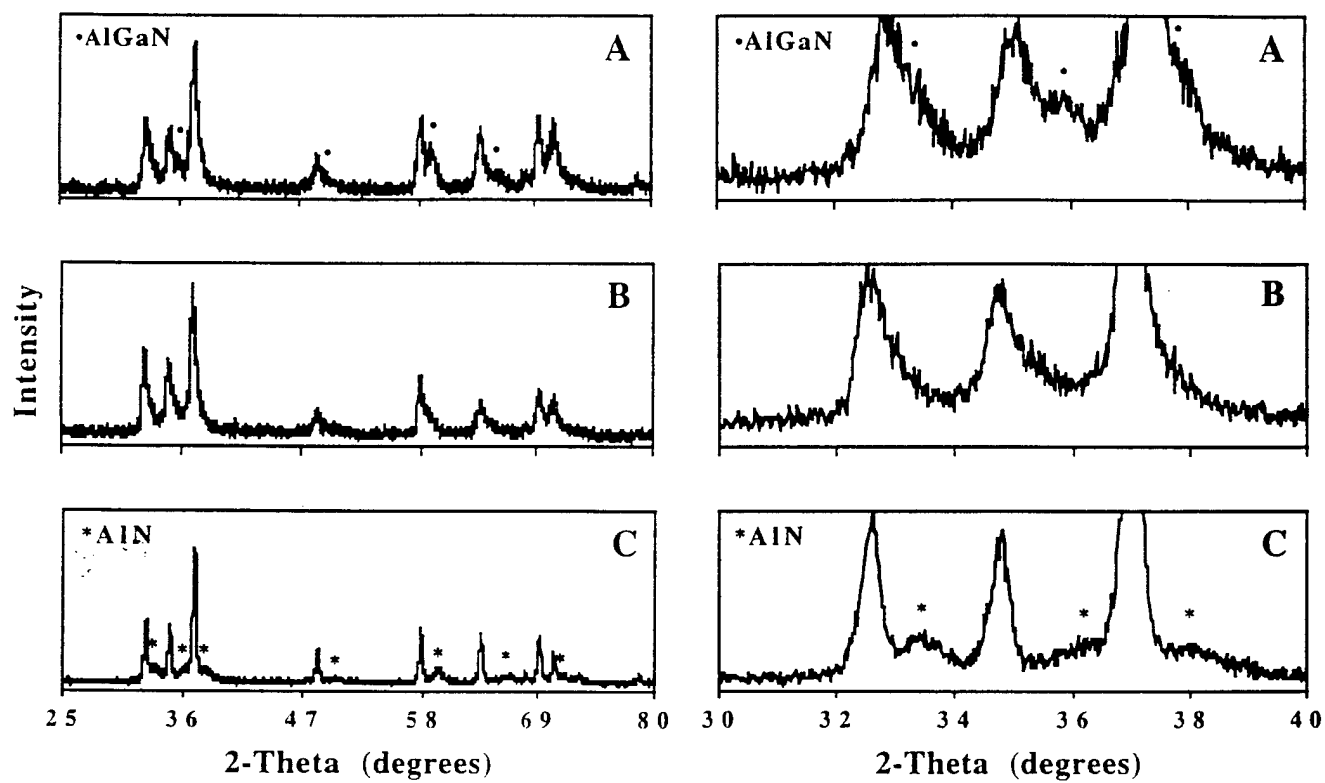
Figure 3. XRD patterns for composites obtained from precursor 4 at different pyrolysis temperatures: (A) 700 °C; (B) 900 °C; (C) 1100 °C (AlGa₂N stands for aluminum/gallium nitride solid solution phase).

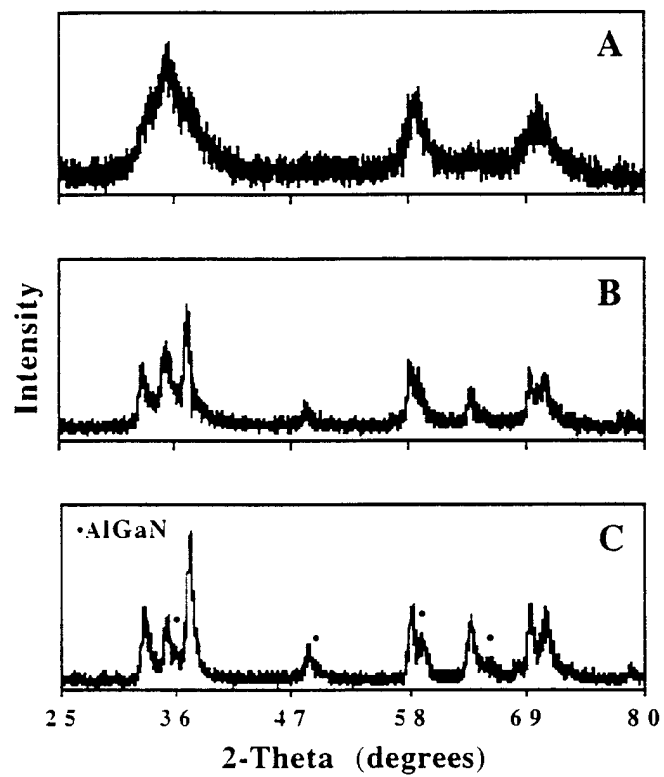
Figure 4. TEM images and electron diffraction pattern for composites obtained from precursor 4 at pyrolysis temperatures: (A) (top row), 700 °C: electron diffraction pattern (left) and HRTEM showing lattice fringes (right). (B) (middle row), 900 °C: low magnification (left) and high magnification of the small particle region (right). (C) (bottom row), 1100 °C: high magnification (left) and HRTEM showing lattice fringes (right) of the small particle region.

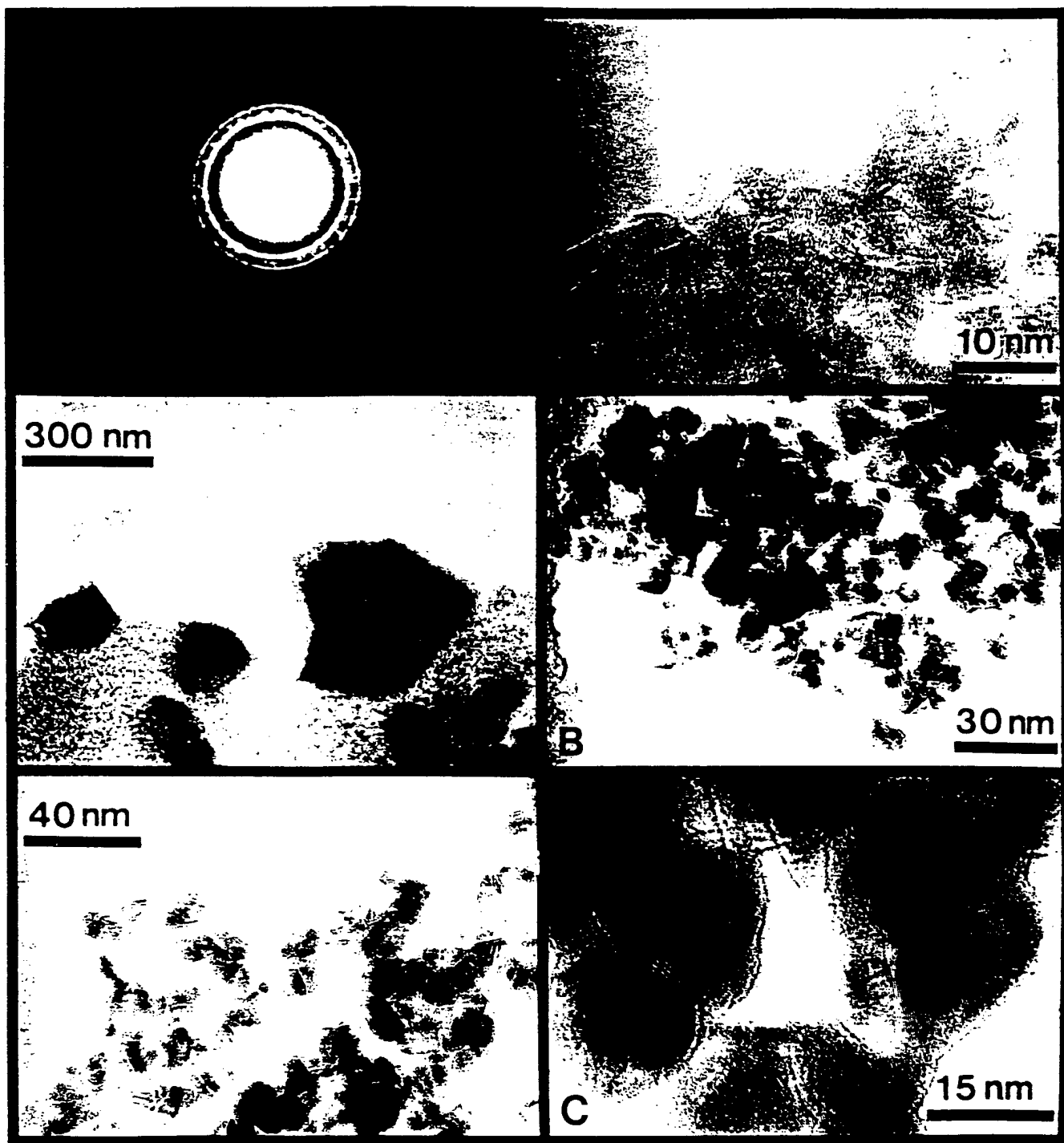
Figure 5. TEM image (top) and electron diffraction patterns (bottom left, small particles; bottom right, large crystallite) for composite from pyrolysis of precursor 3 at 1100 °C.

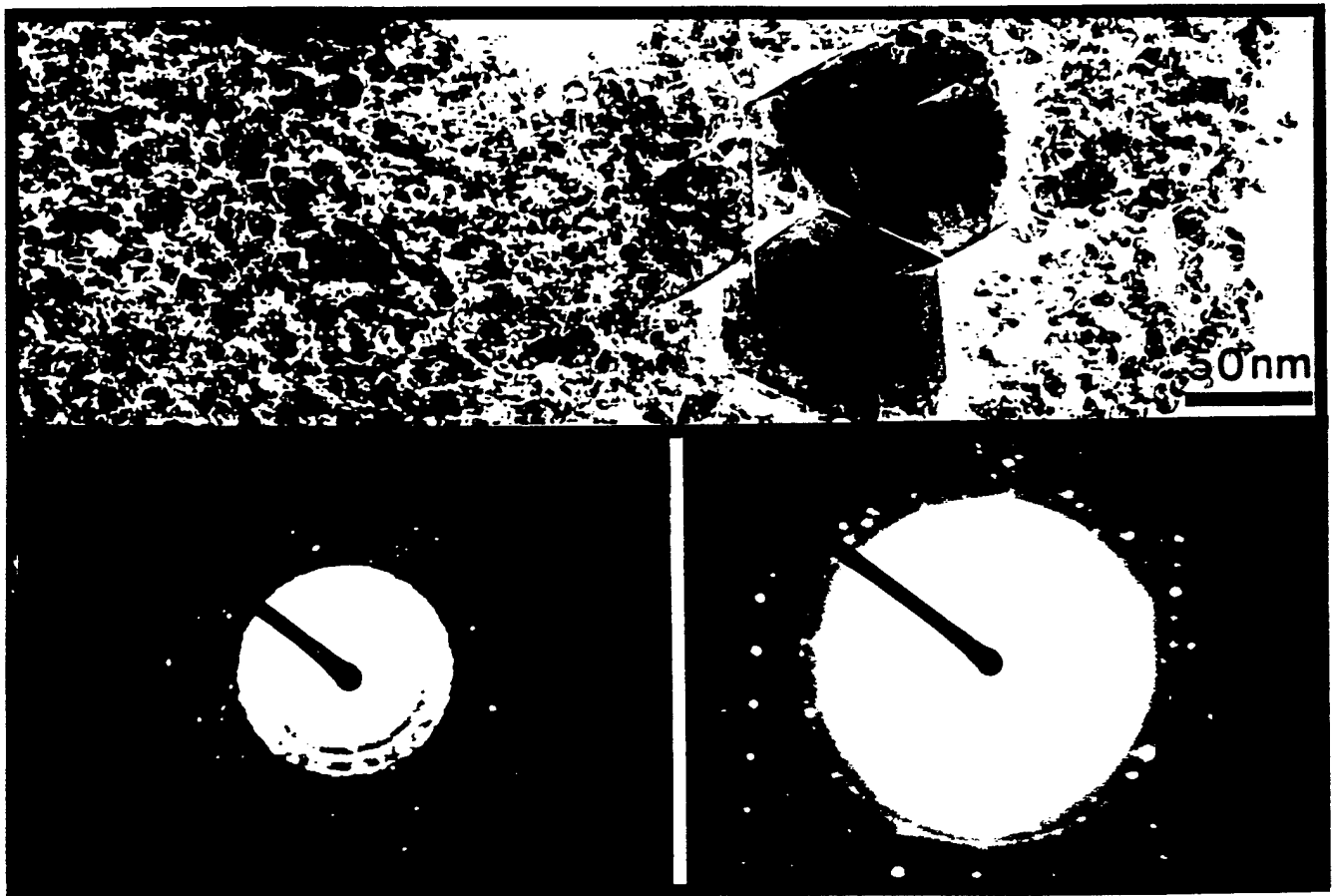
Figure 6. Room temperature photoluminescence spectra at 325 nm excitation wavelength for composites obtained from precursors 1 (A) and 4 (B).











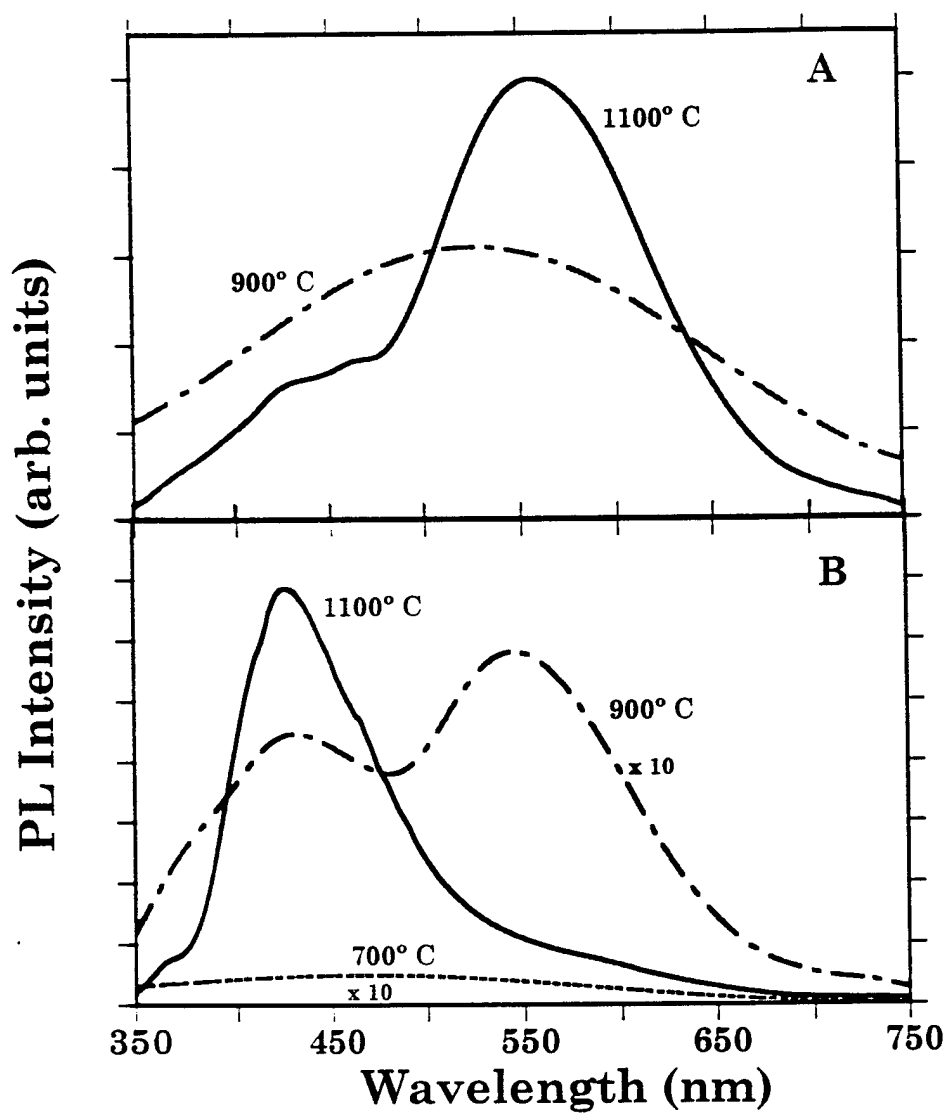


Fig 6

TECHNICAL REPORTS DISTRIBUTION LIST

ORGANOMETALLIC CHEMISTRY FOR ELECTRONIC & OPTICAL MATERIALS

Dr. Harold E. Guard
Code 1113
Chemistry Division, 331
Office of Naval Research
800 N. Quincy Street
Arlington, VA 22217-5660

Defense Technical Information
Center (DTIC)
Ft. Belvoir Headquarters Complex
8725 John J. Kingman Road
STE 0944
Ft. Belvoir, VA 22060

Dr. James S. Murday
Chemistry Division, Code 6100
Naval Research Laboratory
Washington, DC 20375-5320

Dr. John Fischer, Director
Chemistry Division, C0235
Naval Naval Air Weapons Center
Weapons Division
China Lake, CA 93555-6001

Dr. Richard W. Drisko
Naval Facilities & Engineering
Service Center
Code L52
Port Hueneme, CA 93043

Dr. Eugene C. Fischer
Code 2840
Naval Surface Warfare Center
Carderock Division Detachment
Annapolis, MD 21402-1198

Dr. Bernard E. Doua
Crane Division
Naval Surface Warfare Center
Crane, IN 47522-5000

Dr. Peter Seligman
Naval Command, Control and
Ocean Surveillance Center
RDT&E Division
San Diego, CA 93152-5000